A molecular dynamics study of the thermodynamic properties of liquid Ni using the Voter and Chen version of the embedded atom model

M. M. G. Alemany, C. Rey, and L. J. Gallego

Citation: The Journal of Chemical Physics **109**, 3568 (1998); doi: 10.1063/1.476952
View online: http://dx.doi.org/10.1063/1.476952
View Table of Contents: http://scitation.aip.org/content/aip/journal/jcp/109/9?ver=pdfcov
Published by the AIP Publishing

A molecular dynamics study of the thermodynamic properties of liquid Ni using the Voter and Chen version of the embedded atom model

M. M. G. Alemany, C. Rey, and L. J. Gallego
Departamento de Física de la Materia Condensada, Facultad de Física, Universidad de Santiago de Compostela, E-15706 Santiago de Compostela, Spain

(Received 26 February 1998; accepted 1 June 1998)

Using the Voter and Chen version of the embedded atom model, we performed molecular dynamics simulations to compute the thermodynamic properties of liquid Ni up to 3000 K, i.e., well above the melting temperature. Our results show good general agreement with available experimental data. Comparison between simulated and experimental heat capacities requires subtraction from the latter of the electronic contribution, which for liquid transition metals is usually an order of magnitude greater than for simple metals. © *1998 American Institute of Physics.* [S0021-9606(98)51533-4]

I. INTRODUCTION

The embedded atom model (EAM), originally proposed by Daw and Baskes,[1] has been proven to be a powerful tool for investigation of the bulk and surface properties of the late transition and noble metals and their alloys.[2] It has also recently been used to describe the behavior of free and supported metal clusters (see, e.g., Refs. 3–6 and those cited therein). In the EAM, the total energy of the system is considered to be the sum of the energy due to core-core interactions and the energy required to embed each atom in the local electron density created by the remaining atoms (the ''embedding energy''). Although both contributions can be calculated from first principles,[2,7] in practice they are generally obtained by fitting the model to basic solid properties (the lattice constant, cohesive energy, elastic constants and vacancy formation energy) while requiring that the total energy match the ''universal'' equation of state proposed by Rose *et al.*;[8] when the EAM is applied to clusters of transition metals it is advantageous for properties of the diatomic molecule also to be included among the data to which the model is fitted.[3]

Application of the EAM to liquid metals, which exhibit electron densities and atomic spacings different from those of solids, provides a stringent test of the forms chosen for the energy functions and of the method used for their parametrization. In the first such application,[9] a molecular dynamics (MD) study afforded values for the static structure factors of the late transition and noble metals that were in good agreement with experimental data. The static structure and thermodynamic properties of these kinds of liquid metal have in fact subsequently been studied using a variety of different EAM approaches.[10–15] For instance, Holender[11] performed MD studies of solid and liquid transition and noble metals using the Finnis and Sinclair many-body potential,[16] an adaptation of the EAM; Bhuiyan, Silbert and Stott[14] used EAM-based effective pair potentials in conjunction with the variational modified hypernetted chain theory[17] to compute the static structure factors and thermodynamic properties of liquid $3d$, $4d$ and $5d$ transition metals; and Sadigh and Grimvall[15] performed MD simulations to calculate the heat capacities, thermal expansion and compressibility of liquid Cu up to about 3300 K using the Foiles, Baskes and Daw (FBD) version of the EAM.[18]

Recently,[19] we performed a MD study of the dynamical behavior of liquid Ni using the EAM proposed by Voter and Chen (VC),[20] which differs from the widely used FBD model in two main ways: a) its core-core pair interaction has a medium-range attractive contribution, rather than being entirely repulsive; and b) properties of the diatomic molecule as well as bulk solid properties were used in fitting the embedding function and pair interaction. Our computed values of the dynamic structure factor of liquid Ni were in good agreement with the results of inelastic neutron scattering experiments, and the values of the shear viscosity obtained by various methods were also in keeping with available experimental data. However, whether the VC EAM is also capable of describing the thermodynamic properties of liquid transition metals was left unsettled; it is not obvious that a potential derived from properties of the diatomic molecule and properties of the solid measured at a single temperature can correctly describe the temperature-dependent properties of the liquid phase.

To elucidate this question we have carried out a MD simulation study of the thermodynamic properties of liquid Ni up to 3000 K using the VC EAM. In Sec. II we sketch the computational procedure used in this work. More specific details of the calculation of thermodynamic properties, for some of which experimental information is available, are indicated in Sec. III, where we present and discuss our results. Finally, in Sec. IV, we summarize our main conclusions.

II. DETAILS OF THE COMPUTATIONAL METHOD

Using the VC EAM (Ref. 20) we performed MD simulations to study the thermodynamic properties of bulk Ni at constant near-zero pressure and several temperatures in the range 1600–3000 K. Although our main interest is in liquid Ni, calculations were also carried out for the solid phase in order to obtain a melting temperature for comparison with the experimental melting temperature, 1726 K.[21] The same VC EAM potential was used to describe interatomic interac-

tions in both the solid and liquid states, despite their very different interatomic separation distributions. We considered a system of $N=500$ atoms in a cubic box of length L with periodic boundary conditions. The cutoff distance of the VC potential for Ni, $r_{cut}=4.7895$ Å,[20] is smaller than the maximum value allowed by the periodic boundary conditions, $L/2$ [for a fcc arrangement of the N atoms at their 0 K ideal bulk positions $L_0/2=a_0(N/4)^{1/3}/2=8.8$ Å, where $a_0=3.52$ Å is the lattice parameter,[21] and for the high temperatures considered in our study the situation is even more favorable]; hence the full contribution of the potential energy was taken into account in the calculations.

The computational procedure was as follows. First, we performed simulations at zero pressure and several temperatures using the Nosé constant-pressure, constant-temperature (NPT) technique,[22] in which the length of the simulation box, L, is an additional dynamical variable. The equations of motion were solved using a fourth-order Gear predictor-corrector algorithm[23] with a time step $\Delta t_1=5\times10^{-4}$ ps. Two sets of NPT simulations were carried out: a) within the range 1600−2000 K (which includes the experimental melting point), we performed simulations at temperatures separated by 10 K (and additionally at 1705, 1773 and 1873 K), starting in each case from a fcc configuration of the corresponding temperature; b) within the range 2000–3000 K we started from an initial fcc configuration at $T=3000$ K and reduced the temperature gradually by steps of 50 K. At selected temperatures in each range we calculated the energy of the system and the length of the simulation box by averaging over 2×10^4 time steps after an initial equilibration period of at least 2×10^4 time steps. Then, starting from configurations with energies very close to the average values obtained as above, and using cubic boxes of lengths very close to the values calculated above, microcanonical (NVE) MD simulations were carried out using the velocity Verlet algorithm[23] with a time step $\Delta t_2=5\times10^{-3}$ ps (NVE simulations are better than NPT simulations for studying the thermodynamic properties of the system because of the difficulty of controlling the ''mass'' variables in the Nosé method[22]). After an appropriate initial equilibration period, the properties of interest were averaged within each of five successive runs of 2×10^4 time steps.

III. RESULTS

A. Melting temperature and radial distribution function

For each temperature in the range 1600–2000 K, four independent NPT simulations were performed, in each of which the particles were assigned random initial velocities. The melting temperature of Ni was computed by monitoring, in each such simulation, the translational order parameter[23]

$$\overline{\rho}(q)=\frac{1}{3N}\sum_{j=1}^{3}\sum_{i=1}^{N}\cos(\mathbf{q}_j\cdot\mathbf{r}_i), \tag{1}$$

where $\mathbf{r}_i$ is the position vector of atom i and the $\mathbf{q}_j$ are reciprocal lattice vectors of the initial fcc configuration [$\mathbf{q}_1=(2\pi/a)(-1,1,1)$, $\mathbf{q}_2=(2\pi/a)(1,-1,1)$ and $\mathbf{q}_3=(2\pi/a)(1,1,-1)$, where $a=L/(N/4)^{1/3}$]. For a solid $\overline{\rho}(q)$ is of the order of unity, whereas for a liquid it oscillates about zero. The system exhibited a solid structure in all four simulations at 1600 K, 1610 K and 1620 K, and a liquid structure in all four simulations at $T\geqslant1790$ K, but in the range 1620 K $<T<1790$ K the type of structure observed depended on the initial velocity distribution. We took the midpoint of this range, 1705 K, as the calculated melting temperature (estimated error ±85 K); this value is in good agreement with the experimental value 1726 K.[21] Figure 1 shows the evolution of $\overline{\rho}(q)$ at this temperature.

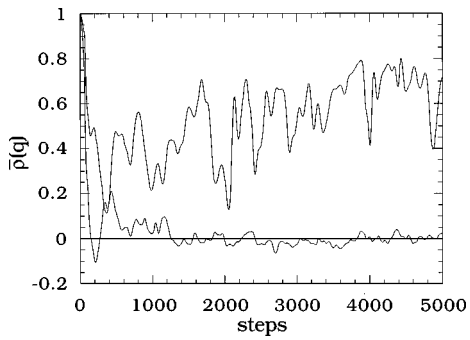

FIG. 1. Time dependence of the translational order parameter $\overline{\rho}(q)$ of liquid Ni at $T=1705$ K, as observed in two simulations with different initial velocity assignments. The upper curve corresponds to a solid structure and the lower curve to a liquid structure.

Figure 2 shows the box length L, in units of L_0, as a function of temperature. Of the two values for each temperature in the range 1620 K$<T<$1790 K, the greater corresponds to the liquid state. The percentage volume change on melting, $\Delta V=100\times[V_l(1705\ \mathrm{K})-V_s(1705\ \mathrm{K})]/V_s(1705\ \mathrm{K})$, is 5.87%, which lies between the two reported experimental values 4.5% (Ref. 21) and 6.3% (Ref. 24). The computed molar volume of liquid Ni at the melting point is $V_l(1705\ \mathrm{K})=7.74\times10^{-6}$ m^3/mol; the experimental result is 7.43×10^{-6} m^3/mol.[24]

Figure 3 shows the radial distribution function [computed from a histogram of the $N(N-1)/2$ particle-particle distances in the simulation box] as a function of $r'=r/a$ at three selected temperatures, 1620 K, 1705 K and 1790 K. Dashed lines represent coordination zones for the ideal fcc structure. At $T=1620$ K, $g(r')$ has peaks at or near some

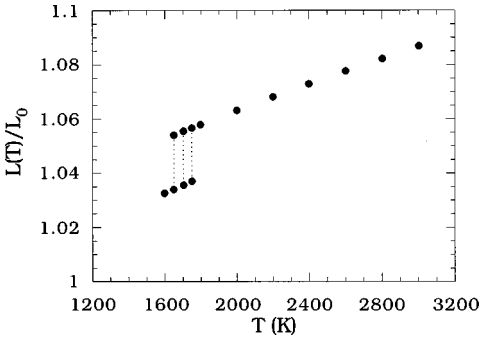

FIG. 2. Box length L (in units of L_0, the length at 0 K) at selected temperatures. Dashed lines join the two values of L, corresponding to different initial velocity assignments, that are observed at each temperature in the range 1620 K $<T<$1790 K.

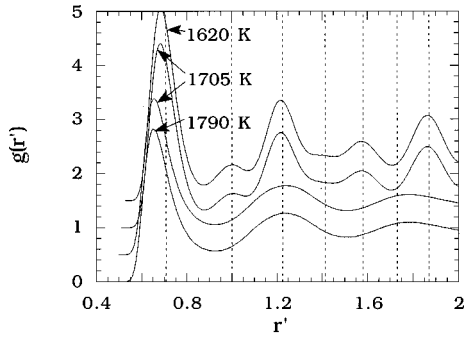

FIG. 3. Calculated radial distribution function $g(r')$ of bulk Ni at several temperatures. Dashed lines denote coordination zones for the ideal fcc structure. The *y*-coordinates are correct for the $T=1790$ K curve; for clarity, the other curves are shifted up by 0.5 (1705 K, lower curve), 1.0 (1705 K, upper curve) or 1.5 (1620 K).

of the ideal fcc positions (although the peaks are lower and broader than those that would be obtained at low temperature), whereas at $T=1790$ K the behavior of $g(r')$ is typical of the liquid state. At $T=1705$ K both structures are observed, in keeping with the results of Fig. 1. In Fig. 4 the simulated radial distribution function $g(r)$ of liquid Ni at $T=1873$ K is compared with the neutron scattering and x-ray results obtained at this temperature by Johnson *et al.*[25] and Waseda[26] respectively. The agreement between the simulated and experimental data is satisfactory, bearing in mind that overestimation of the amplitude of the first $g(r)$ peak is probably inevitable with a potential parametrized on the basis of solid-state properties. As was shown in Ref. 19, the static structure factor $S(q)$ computed for liquid Ni using the VC EAM compares equally well with the experimental results.[26]

B. Heat capacities

The heat capacity of liquid Ni at constant pressure was computed as $C_P=\partial H/\partial T$, where the enthalpy H was obtained from the microcanonical MD simulations as the average

$$\langle H\rangle = E+\langle P\rangle V, \tag{2}$$

E being the total energy. Figure 5 shows that the calculated function $H(T)$ is linear, as was also found by Sadigh and Grimvall[15] in their MD study of liquid Cu using the FBD EAM. The value of C_P given by the slope of this function is $C_P/(Nk)=3.610\pm 0.005$.

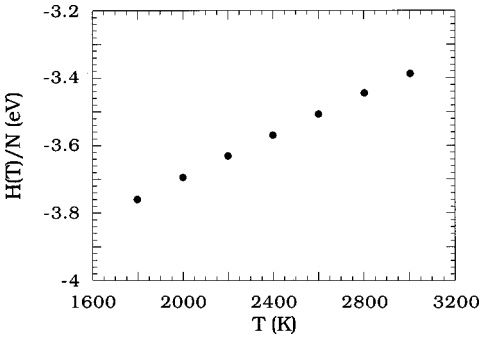

FIG. 5. Temperature dependence of the enthalpy H of liquid Ni, as obtained from our MD simulations.

The heat capacity at constant volume was obtained using the expression[27]

$$C_V=\frac{k}{1+(2/\mu-1)\langle E_{\rm kin}\rangle\langle E_{\rm kin}^{-1}\rangle}, \tag{3}$$

where k is the Boltzmann constant, $E_{\rm kin}$ is the total kinetic energy, and $\mu=3N-3$ is the number of degrees of freedom of the system (in MD simulations the total linear momentum is fixed). Figure 6 shows C_V as a function of T. At temperatures near the critical point (estimated using Lang's formula[28] at about 10 600 K), C_V must asymptotically approach $2Nk$;[29] this behavior has been observed in the low-melting metals Na, K and Hg,[30] and has been related to the gradual disappearance of phonon-like transverse excitations in liquid systems.[29]

Comparison of our computed values of C_P and C_V with available experimental data requires allowance to be made for the electronic contribution, a term that has been ignored is some previous EAM studies of the thermodynamic properties of liquid transition metals (see, e.g., Ref. 11). For this kind of system the inclusion of this contribution is vital, since it is usually an order of magnitude greater than for simple metals.[31] To first order in T,[15,31]

$$C_{P,\rm el}\approx C_{V,\rm el}\approx \tfrac{1}{3}\pi^2 n(E_F)k^2T, \tag{4}$$

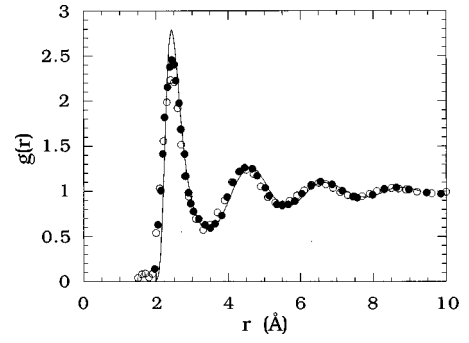

FIG. 4. Radial distribution function $g(r)$ for liquid Ni at $T=1873$ K. The solid line represent our MD results, the black points neutron scattering measurements (Ref. 25) and the white points x-ray diffraction data (Ref. 26).

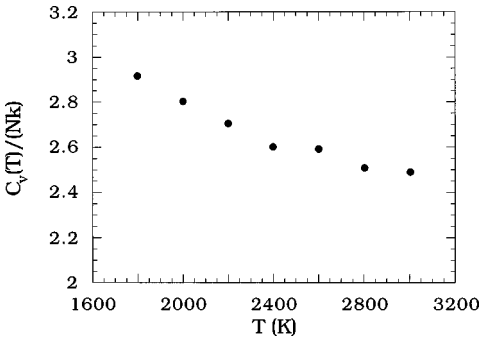

FIG. 6. Temperature dependence of the heat capacity C_V of liquid Ni, as obtained from our MD simulations.

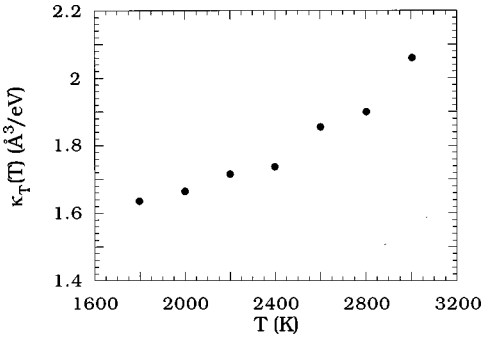

FIG. 7. Temperature dependence of the isothermal compressibility K_T of liquid Ni, as obtained from our MD simulations.

where $n(E_F)$ is the density of electron states (two per orbital) at the Fermi level. Theoretical calculations of $n(E_F)$ for liquid Ni (Ref. 32) lead to the value $C_{P,\mathrm{el}}=1.51\ Nk$ at $T=1773$ K,[33] and subtraction of this quantity from the experimental C_P value, 5.183 Nk,[34] affords $(C_{P,\mathrm{exp}}-C_{P,\mathrm{el}})/(Nk)=3.673$, in good agreement with our calculated value for $C_P/(Nk)$, 3.610 ± 0.005. Similarly, the value $(C_{V,\mathrm{exp}}-C_{V,\mathrm{el}})/(Nk)=2.95$, where $C_{V,\mathrm{exp}}$ is the experimental heat capacity at constant volume for liquid Ni at $T=1773$ K, 4.46 Nk,[33] agrees very well with the value of $C_V/(Nk)$ obtained by simulation at this temperature, 2.90 ± 0.08.

C. Compressibility and adiabatic speed of sound

The isothermal compressibility K_T was obtained from our MD simulations using the expression[19]

$$\frac{1}{K_T}=\frac{N}{\rho}\left(1-\frac{\mu}{2}\right)(\langle E_V^2E_{\mathrm{kin}}^{-1}\rangle-2\langle E_V\rangle\langle E_VE_{\mathrm{kin}}^{-1}\rangle+\langle E_V\rangle^2\langle E_{\mathrm{kin}}^{-1}\rangle)+\rho kT\left(1+2\gamma-\frac{Nk}{C_V}\right)+\frac{N}{\rho}\langle E_{VV}\rangle-\frac{2}{\mu Vk}\langle E_{\mathrm{kin}}\rangle C_V\gamma^2, \tag{5}$$

where ρ is the number density, E_V and E_{VV} are respectively the first and second volume derivatives of the energy, and the Grüneisen parameter γ is given by

$$\gamma=\frac{Nk}{C_V}+\frac{N}{\rho}\left(\frac{\mu}{2}-1\right)(\langle E_V\rangle\langle E_{\mathrm{kin}}^{-1}\rangle-\langle E_VE_{\mathrm{kin}}^{-1}\rangle). \tag{6}$$

Figure 7 shows the calculated K_T as a function of T. The value computed for $T=1773$ K, $(1.00\pm0.03)\times10^{-11}$ m^2/N, agrees very well with the reported experimental value at this temperature, 0.98×10^{-11} m^2/N.[33] The adiabatic compressibility K_S can be obtained from K_T using the expression

$$K_S=\frac{C_V}{C_P}K_T, \tag{7}$$

and the adiabatic speed of sound, c_s, from[35]

$$c_s=\sqrt{\frac{1}{\rho mK_S}}, \tag{8}$$

where m is the atomic mass. The computed value of c_s at $T=1705$ K, 4173 ± 6 m/s, is in good agreement with the reported experimental values, 4045 m/s and 4036 m/s.[24]

IV. CONCLUSIONS

The MD results reported in this paper show that the VC EAM gives a good description of the thermodynamic properties of liquid Ni. In particular, the prediction that the heat capacity C_P is independent of temperature over a wide range of temperatures above the melting point agrees with the experimental findings.[34] Similar behavior has recently been found by Sadigh and Grimvall[15] in a MD study of liquid Cu up to about 3300 K using the FBD EAM, which is also in keeping with experimental measurements. Thus the thermodynamic properties of both transition and noble metals in the liquid phase can be described, even at high temperatures, by EAM approaches with embedding functions and pair interactions parametrized using one-temperature properties of the solid phase (and, in the case of the VC EAM version used here, the properties of the diatomic molecule). Comparison between the simulated and experimental heat capacities of liquid Ni requires that the electronic contribution be taken into account; this contribution has been ignored in some of the previous EAM studies of the thermodynamic properties of liquid transition metals.

ACKNOWLEDGMENTS

This work was supported by the DGICYT, Spain (Project PB95-0720-C02-02) and the Xunta de Galicia (Project XUGA20606B96).

[1] M. S. Daw and M. I. Baskes, Phys. Rev. Lett. **50**, 1285 (1983); Phys. Rev. B **29**, 6443 (1984).
[2] M. S. Daw, S. M. Foiles, and M. I. Baskes, Mater. Sci. Rep. **9**, 251 (1993).
[3] C. Rey, L. J. Gallego, J. García-Rodeja, J. A. Alonso, and M. P. Iñiguez, Phys. Rev. B **48**, 8253 (1993).
[4] C. Rey, J. García-Rodeja and L. J. Gallego, Phys. Rev. B **54**, 2942 (1996).
[5] A. F. Wright, M. S. Daw, and C. Y. Fong, Phys. Rev. B **42**, 9409 (1990).
[6] M. C. Fallis, M. S. Daw, and C. Y. Fong, Phys. Rev. B **51**, 7817 (1995).
[7] M. S. Daw, Phys. Rev. B **39**, 7441 (1989).
[8] J. H. Rose, J. R. Smith, F. Guinea, and J. Ferrante, Phys. Rev. B **29**, 2963 (1984).
[9] S. M. Foiles, Phys. Rev. B **32**, 3409 (1985).
[10] J. B. Adams and S. M. Foiles, Phys. Rev. B **41**, 3316 (1990).
[11] J. M. Holender, Phys. Rev. B **41**, 8054 (1990); J. Phys.: Condens. Matter **2**, 1291 (1990).
[12] L. M. Holzman, J. B. Adams, S. M. Foiles, and W. N. G. Hitchon, J. Mater. Res. **6**, 298 (1991).
[13] R. LeSar, R. Najafabadi, and D. J. Srolovitz, J. Chem. Phys. **94**, 5090 (1991).
[14] G. M. Bhuiyan, M. Silbert, and M. J. Stott, Phys. Rev. B **53**, 636 (1996).
[15] B. Sadigh and G. Grimvall, Phys. Rev. B **54**, 15742 (1996).
[16] M. W. Finnis and J. E. Sinclair, Philos. Mag. A **50**, 45 (1984).
[17] Y. Rosenfeld, J. Stat. Phys. **42**, 437 (1986).
[18] S. M. Foiles, M. I. Baskes, and M. S. Daw, Phys. Rev. B **33**, 7983 (1986).
[19] M. M. G. Alemany, C. Rey, and L. J. Gallego, Phys. Rev. B **58**, 685 (1998).
[20] A. F. Voter and S. P. Chen, in *Characterization of Defects in Materials*, MRS Symposia Proceedings No. 82, edited by R. W. Siegel, J. R. Weertman, and R. Sinclair (Materials Research Society, Pittsburgh, 1987), p. 175.
[21] *Smithells Metals Reference Book*, edited by E. A. Brandes and G. B. Brook (Butterworth–Heinemann, Oxford, 1992).
[22] S. Nosé, Mol. Phys. **52**, 255 (1984).
[23] M. P. Allen and D. J. Tildesley, *Computer Simulation of Liquids* (Oxford

University, Oxford, 1990).
[24] T. Iida and R. I. L. Guthrie, *The Physical Properties of Liquid Metals* (Clarendon, Oxford, 1988).
[25] M. W. Johnson, N. H. March, B. McCoy, S. K. Mitra, D. I. Page, and R. C. Perrin, Philos. Mag. **33**, 203 (1976).
[26] Y. Waseda, *The Structure of Noncrystalline Materials* (McGraw–Hill, New York, 1980).
[27] E. M. Pearson, T. Halicioglu and W. A. Tiller, Phys. Rev. A **32**, 3030 (1985).
[28] G. Lang, Z. Metallkd. **68**, 213 (1977).
[29] D. C. Wallace, B. L. Holian, J. D. Johnson, and G. K. Straub, Phys. Rev. A **26**, 2882 (1982).
[30] G. Grimvall, Phys. Scr. **11**, 381 (1975).
[31] W. H. Young, in *Liquid Metals, 1976* (Institute of Physics, Bristol and London, 1977), p. 1.
[32] S. Asano and F. Yonezawa, J. Phys. F **10**, 75 (1980).
[33] T. Itami and M. Shimoji, J. Phys. F **14**, L15 (1984).
[34] I. Barin, *Thermochemical Data of Pure Substances* (VCH, Weinheim, 1989).
[35] J. M. Haile, *Molecular Dynamics Simulation* (Wiley, New York, 1992).